



## **Final Draft of the original manuscript**

Kutuzau, M.; Blokhin, A.; Yurkshtovich, Y.; Demyanov, S.; Kalanda, N.; Yarmolich, M.; Serdechnova, M.:

**Structural, magnetic and thermodynamic properties of barium ferromolybdate.**

In: Philosophical Magazine. Vol. 101 (2021) 14, 1699 – 1708.

First published online by Taylor & Francis: 18.05.2021

<https://dx.doi.org/10.1080/14786435.2021.1926566>

# **Structural, magnetic and thermodynamic properties of barium ferromolybdate**

Kutuzau M.D.<sup>1,\*</sup>, Blokhin A.V.<sup>2</sup>, Yurkshtovich Y.N.<sup>2</sup>, Demyanov S.E.<sup>1</sup>, Kalanda N.A.<sup>1</sup>, Yarmolich M.V.<sup>1</sup>, Serdechnova M.<sup>3</sup>

<sup>1</sup>*Scientific and Practical Materials Research Centre of the National Academy of Sciences of Belarus, Minsk, 220072 Belarus*

<sup>2</sup>*Belarusian State University, Chemistry Faculty, Minsk, 220030 Belarus*

<sup>3</sup>*Institute of Surface Science, Helmholtz-Zentrum Hereon, D-21502 Germany*

\*Author for correspondence, [algerd1514@tut.by](mailto:algerd1514@tut.by)

**Keywords:** barium ferromolybdate, heat capacity, enthalpy, entropy, magnetization, Curie temperature.

**Abstract.** The heat capacity and magnetization of the obtained by the solid-phase method from simple oxides single-phase compound  $\text{Ba}_2\text{FeMoO}_{6-\delta}$ , in which the superstructural ordering of Fe and Mo cations occurs, was studied. The anomalous behavior of the temperature dependences of heat capacity (deviation from Debye  $T^3$  law) and magnetic moment (ZFC mode) is interpreted as the existence of a superparamagnetic state in nanoscale grains. The second  $\lambda$ -type anomaly of heat capacity in the region of 300 K is due to the transition of the compound from the ferrimagnetic to the paramagnetic state. The Curie temperature, determined from the maximum of excess heat capacity in the region, is in good agreement with the Curie temperature obtained from the results of magnetic measurements,  $T_c = 302$  K. Based on the  $\text{Ba}_2\text{FeMoO}_{6-\delta}$  compounds heat capacity data the next thermodynamic functions were calculated: reduced enthalpy, entropy, reduced Gibbs energy. The values of calculated functions in the region of temperature anomalies made it possible to classify such anomalies as second-order phase transitions.

## **Introduction**

The properties of magnetic semimetals with a double perovskite structure attract the attention of researchers due to the fact that it is highly correlated electronic systems with high Curie temperatures ( $T_c$  up to 500 K), large values of negative magnetoresistance at low temperatures, and almost ~100% spin polarization of conduction electrons<sup>1-3</sup>.

Obtaining a single-phase compound with superstructural ordering of cations with reproducible physicochemical properties is very problematic<sup>4-7</sup>. This is due to the presence of uncontrolled defect formation processes in the structure of double perovskite, occurring during its crystallization by the solid-phase method and arising due to the complexity of chemical processes, such as the multistage nature of this process, low kinetics of phase formation, low mobility of iron and molybdenum cations, for example, in compounds of the  $A_2FeMoO_{6\pm\delta}$ . The object of the study is the compound of barium ferromolybdate ( $Ba_2FeMoO_{6-\delta}$ ), which, in comparison with the in details studied  $Sr_2FeMoO_{6-\delta}$ , has important advantages, such as higher values of negative magnetoresistance as well as of saturation magnetization and a significant magnitude of the magnetocaloric effect outside the room temperature range due to a decrease in the Curie temperature with the introduction of barium<sup>11,12</sup>.

The study of the thermodynamic characteristics of the  $Ba_2FeMoO_{6-\delta}$  compound, which are sensitive to various kinds of phase transformations<sup>13,14</sup>, in combination with the study of magnetic properties will make it possible to understand the nature of the magnetic states of the compound and substantiate the prospects for its application as spintronic sensors.

## Experiment

The ceramic sample of  $Ba_2FeMoO_{6-\delta}$  was obtained from a mixture of  $Fe_2O_3$  and  $MoO_3$  oxides of analytical grade purity and  $BaCO_3$  taken in appropriate ratios. The initial mixture was synthesized at 900 °C (4 h) in air and annealed at 1200 °C (10 h) under 5%  $H_2/Ar$  stream. After annealing the sample was slowly cooled (~100 °C/h).

The phase composition and disorder degree were determined using the ICSD–PDF2 (Release 2000) database and PowderCell, FullProf software by the Rietveld technique on the base of the X-ray diffraction (XRD) data. The XRD patterns were obtained by X-ray diffraction method using an Empyrean diffractometer (firm PANalytical) in  $Cu-K\alpha$  radiation at room temperature.

The degree of superstructural ordering of cations of iron and molybdenum ( $P$ ) was calculated using the formula<sup>15,16</sup>(1):

$$P = (2 * SOF - 1) * 100\% \quad (1)$$

where SOF is Seat Occupancy Factor.

The concentration of anti-structural defects ( $n$ ) relative to the ideal lattice was calculated based on the magnitude of the super-structural ordering of iron and molybdenum cations<sup>15,16</sup>(2):

$$n = \frac{100\% - P}{2} \quad (2)$$

Measurement of magnetization  $\text{Ba}_2\text{FeMoO}_{6-\delta}$  in the temperature range 77–400 K and in a magnetic field 0.86 T was carried out using an universal automated device in FC (field cooling) and ZFC (zero field cooling) modes.

The heat capacity at saturation pressure ( $C_{s,m}$ ) of solid  $\text{Ba}_2\text{FeMoO}_{6-\delta}$  was measured in an automatic vacuum adiabatic calorimeter TAU-10 in the temperature range 5 – 370 K.<sup>17,18</sup> The expanded uncertainty ( $k = 2$ ) of the  $C_{s,m}$  measurements is  $0.004 \cdot C_{s,m}$  between 20 and 370 K, then, below 20 K, increasing to not more than  $0.02 \cdot C_{s,m}$  at 5 K as determined in experiments with benzoic acid, sapphire, and copper in Ref.<sup>18</sup> The reproducibility for the heat-capacity measurements is better than  $0.001 \cdot C_{s,m}$ . An iron-rhodium resistance thermometer with  $R_0 = 50 \Omega$  was used for temperature measurements with the standard uncertainty of 0.01 K. A solid sample of the studied compound (3.0948 g, corrected for buoyancy) was loaded into a titanium calorimetric container ( $V \approx 1.1 \text{ cm}^3$ ), which was further degassed in vacuum for 0.5 h (residual pressure of  $\sim 1 \text{ Pa}$ ). Helium at  $p \approx 15 \text{ kPa}$  and  $T = 290 \text{ K}$  was introduced into the inner free space of the container for facilitation of heat transfer during the measurements. The presence of helium sealed in the container was accounted for in the treatment of the experimental data. The ratio of the sample heat capacity to the total (sample + container) one was between 0.25 and 0.35 in the range from 5 to 20 K, between 0.35 and 0.50 in the range of from 20 to 220 K and not less than 0.50 in the remaining temperature range. Heating periods in the experiments varied from 70 to 180 s below 40 K, from 200 to 250 s between 40 and 80 K and were fixed at 400 s above 80 K. Periods of thermal relaxation varied from 50 to 100 s for  $T < 83 \text{ K}$  in the helium region and remained constant at about 150 s for  $T > 77 \text{ K}$  in the nitrogen region and higher. Periods of temperature-drift measurements were from 200 to 250 s in the helium region and 400 s for  $T > 77 \text{ K}$ . Temperature steps of the heat-capacity measurements were 1/20 of the absolute temperature for  $T < 40 \text{ K}$  and from 1.8 to 2.3 K above 40 K. A correction for adjustment of the heat capacity at saturation pressure to the isobaric heat capacity ( $C_{p,m}$ ) was found to be negligible in the entire temperature range studied due to the extremely low vapor pressure of the compound and, therefore, was not taken into consideration. The atomic masses of elements recommended by IUPAC<sup>19</sup> were used to derive the molar mass of the compound ( $522.449 \text{ g} \cdot \text{mol}^{-1}$ ) without taking into account the possible non-stoichiometry of the sample for oxygen.

## Results and Discussion

The analysis of  $\text{Ba}_2\text{FeMoO}_{6-\delta}$  XRD data (Fig. 1) allowed to determine the single-phase nature of powder and to establish the presence of superstructural ordering of Fe and Mo cations (reflex (111)).

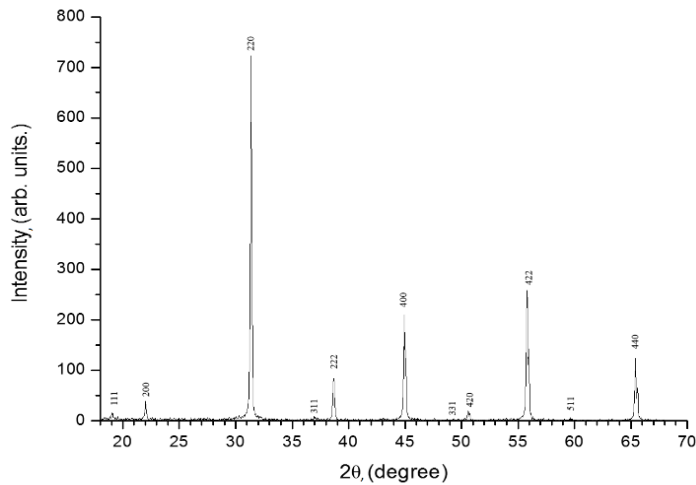


Fig.1  $\text{Ba}_2\text{FeMoO}_{6-\delta}$  XRD pattern.

An important characteristic that determines the functional properties of double perovskites is the concentration of antistructure defects, which can be determined from the ratio of integrated intensities of the diffraction peaks.<sup>20</sup> In the ideal case the iron and molybdenum atoms are staggered in  $\text{Ba}_2\text{FeMoO}_{6-\delta}$  crystal lattice – the superstructural ordering of iron and molybdenum cations. However, it often happens that the iron cation replaces the molybdenum cation, and vice versa (anti-structural defect (ASD)). It is necessary to note that the diffraction peak (111) in the double perovskite structure  $\text{Ba}_2\text{FeMoO}_{6-\delta}$  is superstructural and it is associated with the Fe/Mo alternative ordering. Otherwise the diffraction peak (111) is absent.

The presence of the peak (111) in the diagram (Fig. 1) made it possible to obtain in accordance with equations (1), (2) the following values: SOF = 0.90, P = 80%, n = 10%.

The heat capacity of barium ferromolybdate was measured in the adiabatic calorimeter (Fig. 2) and based on this the thermodynamic functions (reduced enthalpy, entropy, Gibbs reduced energy) of barium ferromolybdate were calculated.

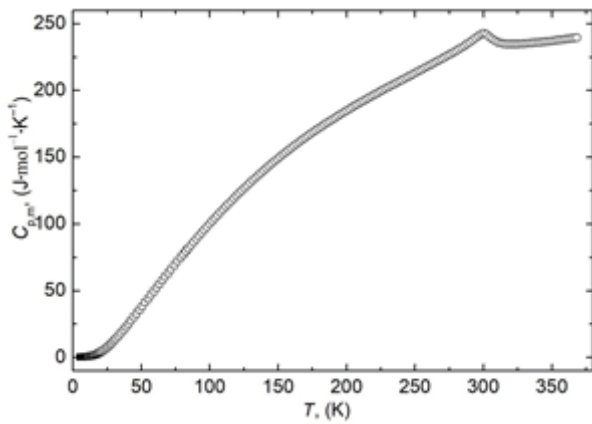


Fig. 2 Temperature dependence of isobaric heat capacities of barium ferromolybdate between (5 and 370) K.

It is obvious that there are two anomalies in this dependence: the peak of the  $C_{p,m}$  value in the range of room temperatures and the deviation from the cubic Bloch law at temperatures below 15 K, confirmed by the dependence of the reduced isobaric heat capacity of barium ferromolybdate on the square of the temperature, Fig. 3.

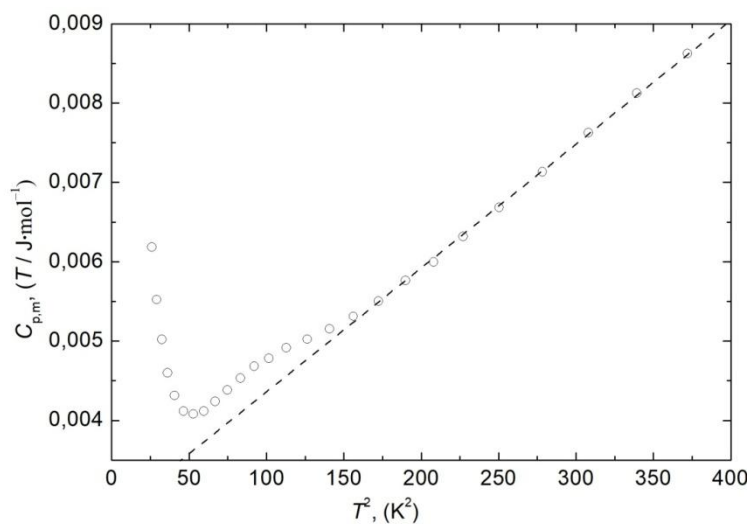


Fig. 3 Dependence of reduced isobaric heat capacity of barium ferromolybdate on the temperature square between (5.1 and 13.1) K (dashed line, a straight line connecting the reduced heat capacities at  $T = 0$  K and  $T = 13.1$  K).

The deviation from the close to linear dependence of the reduced heat capacity on the temperature square begins below  $T = 13.1$  K, and the values of the reduced heat capacity do not tend to zero when the temperature decreases.

The heat capacities of the compound at  $T < 5.1$  K were calculated using the equation (3):

$$C_{p,m} = 0,2087 * T - 6,979 * 10^{-2} * T^2 + 8,460 * 10^{-3} * T^3 - 3,087 * 10^{-4} * T^4 \quad (3)$$

This equation was obtained from the experimental heat capacities in the temperature range of (5.1 to 10.1) K using the least squares method. Such extrapolation of the heat capacity leads to the detection of the anomaly in the low temperature region. As it can be seen in fig. 4, apparently, this anomaly can also be attributed to a second-order phase transition and is determined by a change in the dominant magnetic state.

The heat capacity baseline in the anomaly region (Fig. 4) was described by the equation (4):

$$C_{p,m}(reg) = 8,0280 * 10^{-3} * T + 3,3045 * 10^{-4} * T^3 + 2,3890 * 10^{-7} * T^5 \quad (4)$$

which was derived from the experimental heat capacities of the compound in the temperature range of (13.1 to 31.5) K using the least squares method.

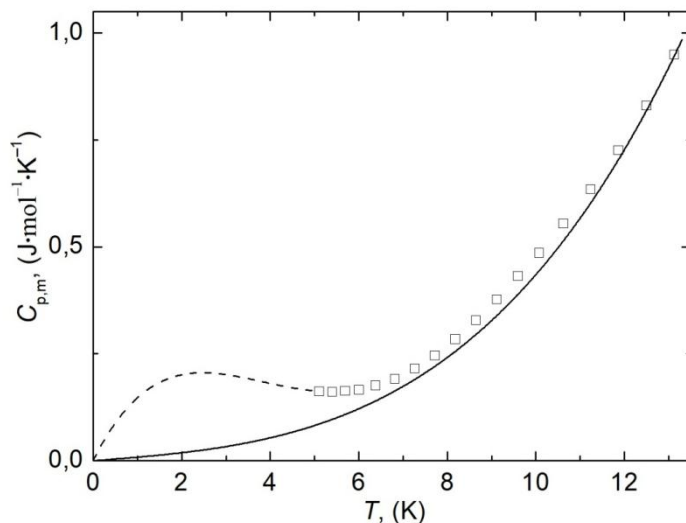


Fig. 4 Temperature dependence of isobaric heat capacity of barium ferromolybdate between (0 and 13) K (dashed line shows extrapolated heat capacity values; solid line is heat capacity baseline).

The excess heat capacity in the anomaly region was calculated according to the equation (5):

$$\Delta_{ex} C_{p,m} = C_{p,m} - C_{p,m}(reg) \quad (5)$$

The values  $C_{p,m}$  are the heat capacities calculated using equation (3) between 0 and 5.1 K and  $C_{p,m}(reg)$  are the experimental heat capacities between 5.1 and 13.1 K. Excess enthalpy and excess entropy of the low-temperature anomaly were obtained by integrating of excess heat capacity and reduced excess heat capacity over temperature respectively and were found to be equal  $\Delta_{ex}H_m = 0,96 \pm 0,03 \text{ (J*mol}^{-1}\text{)}$  and  $\Delta_{ex}S_m = 0,46 \pm 0,02 \text{ (J*K}^{-1}*\text{mol}^{-1}\text{)}$ .

As mentioned above, in the  $\text{Ba}_2\text{FeMoO}_{6-\delta}$  compound an anomaly is observed in the temperature range of 300-320 K. It is caused by the transition of the material from the ferrimagnetic to the paramagnetic state with the corresponding Curie temperature of barium ferromolybdate  $T_c \sim 300$  K, which is proved by the temperature dependence of the excess heat capacity in the region of the high-temperature phase transition of barium ferromolybdate (fig. 5). Based on its shape, this anomaly can be regarded as a  $\lambda$ -type second-order transition. Consequently, it is possible to determine only the excess enthalpy and excess entropy, the temperature dependences of which have no gaps and are to be equal  $\Delta_{ex}H_m = 509 \pm 3$  ( $\text{J}^*\text{mol}^{-1}$ ) and  $\Delta_{ex}S_m = 1,76 \pm 0,01$  ( $\text{J}^*\text{K}^{-1}*\text{mol}^{-1}$ ).

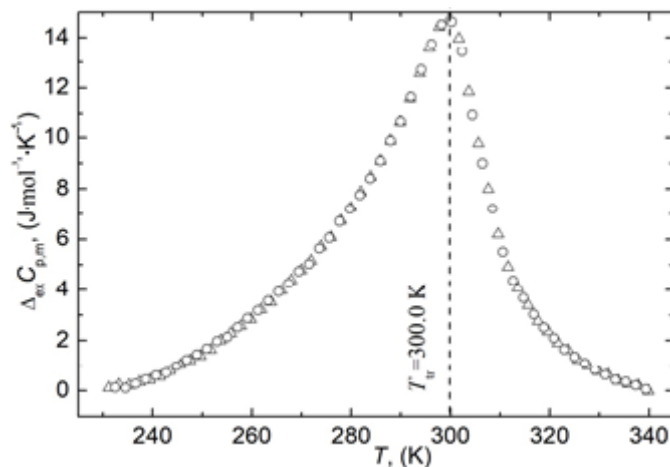


Fig. 5 Temperature dependence of excess heat capacity in the phase transition region of barium ferromolybdate.

The heat capacity baseline in the phase transition region was described by the equation (6):

$$C_{p,m}(\text{reg}) = -82,81 + 2,182 * T - 5,020 * 10^{-3} * T^2 + 3,999 * 10^{-6} * T^3 \quad (6)$$

which was derived from the experimental heat capacities of the compound in the temperature ranges of 200-230 K and 340-370 K using the least squares method. The excess heat capacity in the phase transition interval was calculated as the differences between the experimental heat capacities and the baseline heat capacities according to the equation (5).

The Curie temperature, determined from the maximum of excess heat capacity in the transition regions in such temperature range for the  $\text{Ba}_2\text{FeMoO}_{6-\delta}$  compound, is in good agreement with the Curie temperature obtained from magnetic measurements. As can be seen from Fig. 6, the temperature dependence of the magnetization of the sample  $M^2(T)$  is divided into 2 branches, the first of which (“low temperature”) changes faster with temperature than the second (“high temperature”). The transition point of the “low-temperature” branch to the “high-

temperature” branch lies at  $T \sim 300$  K, which corresponds to the Curie temperature for  $\text{Ba}_2\text{FeMoO}_{6-\delta}$  ( $T_c = 302$  K).

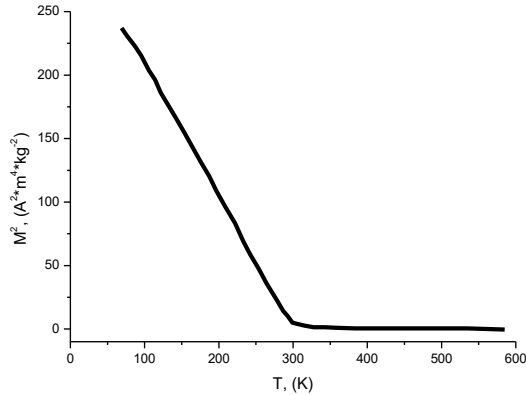


Fig. 6. Temperature dependence  $\text{Ba}_2\text{FeMoO}_{6-\delta}$  of the magnetic moment square

Temperature dependence of  $\text{Ba}_2\text{FeMoO}_{6-\delta}$  magnetic moment (Fig. 7) confirms the presence of anomalies in the low-temperature region.

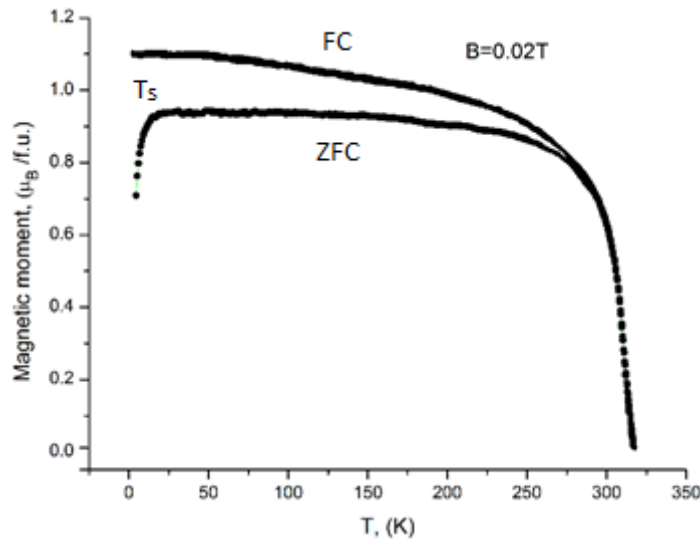


Fig. 7. Temperature dependence of the  $\text{Ba}_2\text{FeMoO}_{6-\delta}$  magnetic moment.

From fig. 7 it can be seen, that when a magnetic field with magnetic induction  $B = 0.02$  T is turned on at  $T = 4.2$  K and then heated to  $T \sim 25$  K (ZFC-branch) it occurs a sharp increase in the magnetic moment of the sample to  $T_s$ . This indicates the transition of nanosized grains to a superparamagnetic state in which exchange forces provide uniform magnetization along the anisotropy axis. The  $T_s$  temperature is critical, delimiting areas with different magnetic states. At this temperature the system goes over to a stable superparamagnetic state, while the ferrimagnetic state still remains metastable and blocked by the energy of magnetic anisotropy.

## Conclusion

Based on the  $\text{Ba}_2\text{FeMoO}_{6-\delta}$  compounds heat capacity data the next thermodynamic functions were calculated: reduced enthalpy, entropy, reduced Gibbs energy. The values of calculated functions in the region of temperature anomalies made it possible to classify such anomalies as second-order phase transitions.

When measuring the heat capacity in the temperature range of 5-30 K, it was found that in the low-temperature region it does not obey the Debye  $T^3$  law and has an anomaly indicating the realization of a superparamagnetic state in double perovskite. It was confirmed by the temperature dependence of the magnetic moment.

The second  $\lambda$ -type anomaly in the region of 300 K is due to the transition of material from ferrimagnetic to paramagnetic state. The Curie temperature, determined from the maximum of excess heat capacity in the region, is in good agreement with the Curie temperature obtained from the results of magnetic measurements,  $T_c = 302$ .

## Acknowledgement

The authors acknowledge a support of the work in frames of the European projects H2020 - MSCA - RISE2017 - 778308 - SPINMULTIFILM and H2020-MSCA-RISE-2018-823942 – FUNCOAT.

## References

1. Hemery E. Magnetic and Transport Studies of Strongly Correlated Perovskite Ceramics. *Victoria Univ Wellington*. 2007; Thesis:112.
2. Serrate D, Teresa JM De, Ibarra MR. Double perovskites with ferromagnetism above room temperature. *J Phys Condens Matter*. 2007;19(2):023201. doi:10.1088/0953-8984/19/2/023201
3. Topwal D, Sarma DD, Kato H, Tokura Y, Avignon M. Structural and magnetic properties of  $\text{Sr}_2\text{Fe}_{1+x}\text{Mo}_{1-x}\text{O}_6$  ( $-1 \leq x \leq 0.25$ ). *Phys Rev B*. 2006;73(9):094419. doi:10.1103/PhysRevB.73.094419
4. Cernea M, Vasiliu F, Bartha C, Plapcianu C, Mercioniu I. Characterization of ferromagnetic double perovskite  $\text{Sr}_2\text{FeMoO}_6$  prepared by various methods. *Ceram Int*. 2014;40(8):11601-11609. doi:10.1016/j.ceramint.2014.03.142
5. Jurca B, Berthon J, Dragoe N, Berthet P. Influence of successive sintering treatments on high ordered  $\text{Sr}_2\text{FeMoO}_6$  double perovskite properties. *J Alloys Compd*. 2009;474(1-2):416-423. doi:10.1016/j.jallcom.2008.06.100
6. Fang T-T, Lin J-C. Formation kinetics of  $\text{Sr}_2\text{FeMoO}_6$  double perovskite. *J Mater Sci*. 2005;40(3):683-686. doi:10.1007/s10853-005-6307-8
7. Huang YH, Lindén J, Yamauchi H, Karppinen M. Simple and Efficient Route to Prepare Homogeneous Samples of  $\text{Sr}_2\text{FeMoO}_6$  with a High

- Degree of Fe/Mo Order. *Chem Mater.* 2004;16(22):4337-4342. doi:10.1021/cm0493288
- 8. Rager J, Zipperle M, Sharma A, MacManus-Driscoll JL. Oxygen Stoichiometry in Sr<sub>2</sub>FeMoO<sub>6</sub>, the Determination of Fe and Mo Valence States, and the Chemical Phase Diagram of SrO-Fe<sub>3</sub>O<sub>4</sub>-MoO<sub>3</sub>. *J Am Ceram Soc.* 2004;87(7):1330-1335. doi:10.1111/j.1151-2916.2004.tb07730.x
  - 9. Klencsár Z, Németh Z, Vértes A, et al. The effect of cation disorder on the structure of Sr<sub>2</sub>FeMoO<sub>6</sub> double perovskite. *J Magn Magn Mater.* 2004;281(1):115-123. doi:10.1016/j.jmmm.2004.04.097
  - 10. Poddar A, Bhowmik RN, Muthuselvam IP, Das N. Evidence of disorder induced magnetic spin glass phase in Sr<sub>2</sub>FeMoO<sub>6</sub> double perovskite. *J Appl Phys.* 2009;106(7):073908. doi:10.1063/1.3236566
  - 11. Turchenko V, Kalanda N, Yarmolich M, Balasoiu M, Lupu N. Features of crystalline and magnetic structure of barium ferromolybdate in a wide temperature range. *J Magn Magn Mater.* 2019;477(August 2018):42-48. doi:10.1016/j.jmmm.2018.12.096
  - 12. Kalanda M, Suchaneck G, Saad A, Demyanov S, Gerlach G. Influence of Oxygen Stoichiometry and Cation Ordering on Magnetoresistive Properties of Sr<sub>2</sub>FeMoO<sub>6±δ</sub>. *Mater Sci Forum.* 2010;637:338-343. doi:10.4028/www.scientific.net/MSF.636-637.338
  - 13. Sankovich AM, Chislova I V, Blokhin A V, Bal'makov MD, Zvereva IA. Low-temperature calorimetric study of layered perovskite-like ferrites GdSrFeO<sub>4</sub> and Gd<sub>2</sub>SrFe<sub>2</sub>O<sub>7</sub>. *J Therm Anal Calorim.* 2016;126(2):601-608. doi:10.1007/s10973-016-5542-3
  - 14. Kohut S V, Sankovich AM, Blokhin A V, Zvereva IA. Low-temperature heat capacity and thermodynamic properties of layered perovskite-like oxides NaNdTiO<sub>4</sub> and Na<sub>2</sub>Nd<sub>2</sub>Ti<sub>3</sub>O<sub>10</sub>. *J Therm Anal Calorim.* Published online 2013:4-11. doi:10.1007/s10973-013-3261-6
  - 15. Huang YH, Karppinen M, Yamauchi H, Goodenough JB. Systematic studies on effects of cationic ordering on structural and magnetic properties in Sr<sub>2</sub>FeMoO<sub>6</sub>. *Phys Rev B.* 2006;73:104408-1-104408-5. doi:10.1103/PhysRevB.73.104408
  - 16. Kalanda N, Turchenko V, Karpinsky D, et al. The Role of the Fe / Mo Cations Ordering Degree and Oxygen Non-Stoichiometry on the Formation of the Crystalline and Magnetic Structure of Sr<sub>2</sub>FeMoO<sub>6 - δ</sub>. *Phys status solidi.* 2018;1800278:1-7. doi:10.1002/pssb.201800278
  - 17. Thermodynamics JC, Kabo GJ, Blokhin A V, et al. Thermodynamic properties of organic substances : Experiment , modeling , and technological applications. *J Chem Thermodyn.* 2019;131:225-246. doi:10.1016/j.jct.2018.10.025
  - 18. Blokhin A V, Paulechka YU, Kabo GJ. Thermodynamic Properties of [ C<sub>6</sub>mim ][ NTf<sub>2</sub> ] in the Condensed State. *J Chem Eng.* 2006; 51:1377-1388.
  - 19. Meija J, Coplen TB, Berglund M, et al. Atomic weights of the elements 2013 ( IUPAC Technical Report ). *Pure Appl Chem.* 2016;88(3):265-291. doi:10.1515/pac-2015-0305

20. Balcells L, Navarro J, Bibes M, Roig A, Martí B, Fontcuberta J. Cationic ordering control of magnetization in Sr<sub>2</sub>FeMoO<sub>6</sub> double perovskite. *Appl Phys Lett.* 2001;78:781-783. doi:10.1063/1.1346624